# **ORIGINAL ARTICLE**



# latrogenic muscle damage in transforaminal lumbar interbody fusion and adjacent segment degeneration: a comparative finite element analysis of open and minimally invasive surgeries

Yogesh Kumaran<sup>1</sup> · Anoli Shah<sup>1</sup> · Akhil Katragadda<sup>1</sup> · Adit Padgaonkar<sup>1</sup> · Joseph Zavatsky<sup>3</sup> · Robert McGuire<sup>4</sup> · Hassan Serhan<sup>2</sup> · Hossein Elgafy<sup>1</sup> · Vijay K. Goel<sup>1</sup>

Received: 18 October 2020 / Revised: 12 May 2021 / Accepted: 24 June 2021 / Published online: 14 July 2021 © The Author(s), under exclusive licence to Springer-Verlag GmbH Germany, part of Springer Nature 2021

#### **Abstract**

**Purpose** Lumbar procedures for Transforaminal Lumbar Interbody Fusion (TLIF) range from open (OS) to minimally invasive surgeries (MIS) to preserve paraspinal musculature. We quantify the biomechanics of cross-sectional area (CSA) reduction of paraspinal muscles following TLIF on the adjacent segments.

**Methods** ROM was acquired from a thoracolumbar ribcage finite element (FE) model across each FSU for flexion-extension. A L4-L5 TLIF model was created. The ROM in the TLIF model was used to predict muscle forces via OpenSim. Muscle fiber CSA at L4 and L5 were reduced from 4.8%, 20.7%, and 90% to simulate muscle damage. The predicted muscle forces and ROM were applied to the TLIF model for flexion-extension. Stresses were recorded for each model.

**Results** Increased ROM was present at the cephalad (L3-L4) and L2-L3 level in the TLIF model compared to the intact model. Graded changes in paraspinal muscles were seen, the largest being in the quadratus lumborum and multifidus. Likewise, intradiscal pressures and annulus stresses at the cephalad level increased with increasing CSA reduction.

**Conclusions** CSA reduction during the TLIF procedure can lead to adjacent segment alterations in the spinal element stresses and potential for continued back pain, postoperatively. Therefore, minimally invasive techniques may benefit the patient.

**Keywords** Transforaminal lumbar interbody fusion (TLIF)  $\cdot$  Open and minimally invasive approaches  $\cdot$  Iatrogenic muscle damage  $\cdot$  Lumbar spine  $\cdot$  Finite element analysis

# Introduction

There has been an increase in lumbar spine fusion procedures to restore spinal alignment and function in low back pain patients. Advancements in lumbar spine fusion procedures including the transforaminal lumbar interbody fusion (TLIF), are typically used for the treatment of a variety of spinal pathologies such as spinal stenosis, spondylolisthesis, and degenerative disc disease [1, 2]. There has been a shift

✓ Vijay K. GoelVijay.Goel@utoledo.edu

- The Engineering Center for Orthopaedic Research Excellence (E-CORE), Toledo, OH, US
- Departments of Bioengineering and Orthopaedic Surgery, University of Toledo, Toledo, OH, US
- <sup>3</sup> Spine and Scoliosis Specialists, Tampa, FL, US
- <sup>4</sup> University of Mississippi Medical Center, Jackson, MS, US

Springer

in TLIF techniques from open (OS) to minimally invasive (MI) with an aim to preserve paraspinal musculature. Both techniques provided long-term improvement in back pain and disability, while minimally invasive TLIF (MITLIF) additionally led to decreased hospital stay, reduced postoperative pain, and accelerated return to work, as compared to open TLIF (OSTLIF), though there is still much debate on which approach is the ideal method [3].

A study by Bresnahan et al. [4] explored the changes that occurred in muscle activity after paraspinal cross sectional area (CSA) reduction in an L3-L5 fusion procedure using a thoracolumbar ribcage model in a dynamic modeling software. The decrease in muscle CSA from intraoperative paraspinal manipulation produced postoperative changes in the muscle activity that were correlated with percent reductions in muscle area. The authors did not explore the biomechanical effects of these changes in muscular forces to understand their role in adjacent segment degeneration (ASD).

From a biomechanical standpoint, the literature on correlation between paraspinal CSA reduction and its effect on adjacent lumbar segments is sparse and thus unclear. We hypothesize that minimization of muscle damage is beneficial by reducing segmental effects adjacent to the index surgical level. We are addressing this issue by utilizing a novel multiprogram approach based on OpenSim Musculoskeletal Modeling (Simbios, California, USA) and Abaqus Finite Element Analysis (Simulia/Dassault Systèmes, Vélizy-Villacoublay, France).

# Methods

#### Intact finite element (FE) model

A non-linear ligamentous finite element model was developed using the CT scans of a 55-year-old healthy adult spine with no abnormalities, deformities, or severe degeneration. This model contained a ribcage, thoracolumbar spine, pelvis and femurs (Fig. 1) and was fixed at the base [29–32].

The vertebral bodies were modelled as a cortical bone shell of 0.5 mm thickness with a core of cancellous bone, both were modelled as a linear elastic isotropic material [29]. The annulus fibrosa was simulated as a composite solid with alternating ±30° collagen fibers modelled using REBAR elements with "no compression" property and the nucleus pulposa was simulated as a linear elastic material [29–31]. The facet joints were modeled using three-dimensional gap elements with an initial defined clearance of 0.5mm. All



**Fig. 1** Human thoracic spine FE model. Femur across the hip joint was fixed and model fixed at the distal end of the femur as well [23, 24]

ligamentous structures were modeled as hypoelastic materials with "tension only" property. The material properties for the human thoracic-pelvis FE model are listed in Table 1 [29–32]. The thoracic spine consisted of 104450 elements and 121045 nodes. The lumbar spine consisted of 49441 elements and 56679 nodes. The pelvis consisted of 31307 elements and 39673 nodes.

Angular range of motion (ROM) for this intact model at each vertebral segment was obtained for a 4Nm moment applied at the T1 endplate [5] (Fig. 2). The validation study was done separately for the thoracic and lumbar region and compared against the literature data [5, 26–33]. The thoracic spine from T1-T12 was previously validated by comparing the motion of the FE model with *in vitro* ROM data [5, 32, 33]. The lumbar spine was previously validated in a number of studies as well [19, 26–33].

#### Instrumented FE model

The intact model was modified to simulate an instrumented model. It involved simulating unilateral facetectomy and resection of the annulus fibrosus at L4-L5 level. The posterior longitudinal ligament was also removed at L4-L5. The nucleus pulposus was resected and a TLIF Polyetherketone (PEEK) cage was modeled with "Tie" interactions on the L4 inferior endplate and L5 superior endplate. The pedicle screw fixation (PSF) with titanium (Ti) rods and titanium alloy (Ti-Alloy) pedicle screws were modeled to further stabilize the L4-L5 functional spine unit (FSU). The material properties and contact properties were assigned based on the literature (Table 1). The segmental flexion and extension thoracic ROM of the intact model were input into the thoracic segments (T1-L1) of the instrumented model. Likewise, the overall lumbar ROM (L1-S1) from the intact model was simulated in the instrumented model at the L1 segment (Fig. 2) [6]. This ROM was used as an input in the OpenSim thoracolumbar model for all muscle reduction cases.

# **Calculation of muscle forces**

Based on post-operative clinical data, paraspinal muscles showed a CSA reduction of 20.7% and 4.8% indicative of postoperative muscle damage in OSTLIF and MITLIF, respectively [7]. 90% CSA reduction indicates complete iatrogenic damage in TLIF (CDTLIF). Our goal was to simulate varying levels of CSA reduction that may occur post and intra-operatively; 4.8%, 20.7%, and 90% reduction cases were simulated in the model. An OpenSim thoracolumbar model was utilized to compute muscle forces as a function of degree of CSA reduction [8]. To simulate muscle damage, the CSA was adjusted via reduction of the maximum



Table 1 Relevant material properties applied to the finite element model obtained from the literature [22–24]

Bony Structure	Material Model / Element Type	Young's Modulus	Poisson's Ratio
Cortical Bone	Isotropic, elastic / hexahedral elements	12000	0.3
Cancellous Bone	Isotropic, elastic / hexahedral elements	100	0.2
Intervertebral disc			
Annulus Ground Substance	Isotropic, Elastic / hexahedral elements	4.2	0.45
Annulus (fibers)	Rebar	357–550	0.3
Nucleus Pulposus	Incompressible, Isotropic, Elastic / hexahedral elements	9	0.4999
Ligaments			
Anterior Longitudinal	Tension-only, Truss elements	7.8(<12%), 20.0(>12%)	0.3
Posterior Longitudinal	Tension-only, Truss elements	10.0(<11%), 20.0(>11%)	0.3
Ligamentum Flavum	Tension-only, Truss elements	15.0(<6.2%), 19.5(>6.2%)	0.3
Intertransverse	Tension-only, Truss elements	10.0(<18%), 58.7(>18%)	0.3
Interspinous	Tension-only, Truss elements	10.0(<14%), 11.6(>14%)	0.3
Supraspinous	Tension-only, Truss elements	8.0(<20%), 15.0(>20%)	
Capsular	Tension-only, Truss elements	7.5(<25%), 32.9(>25%)	0.3
Joint			
Apophyseal Joints	Non-linear Soft contact, GAPPUNI elements	-	_
Instrumentation			
PEEK (Interbody Cage)	Isotropic, elastic / hexahedral elements	3500	0.3
Titanium (Rods)	Isotropic, elastic / hexahedral elements	120,000	0.3
Pedicle Screws (Ti-Alloy)	Isotropic, elastic / hexahedral elements	110,000	0.3

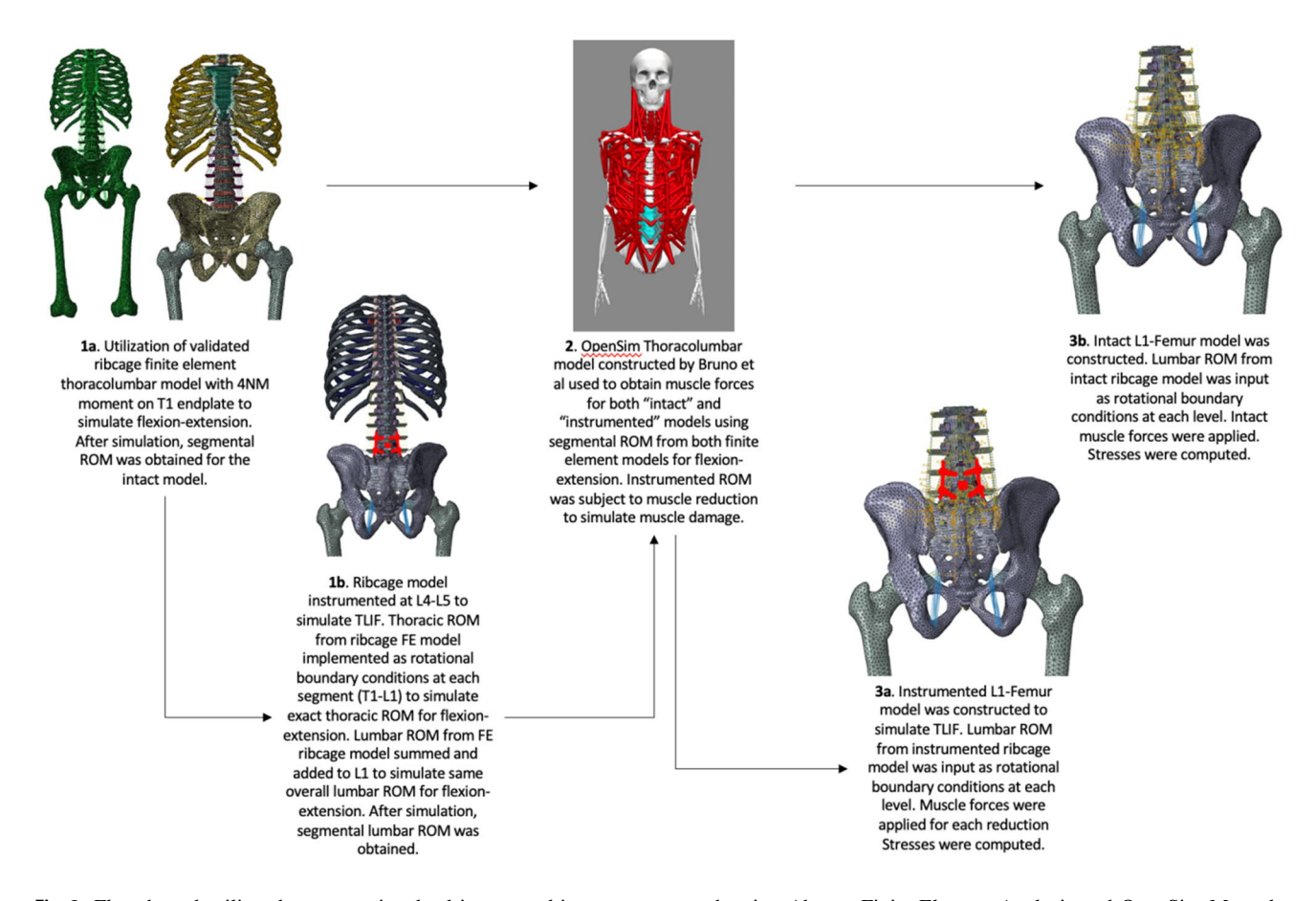


Fig. 2 Flowchart detailing the process involved in our multiprogram approach using Abaqus Finite Element Analysis and OpenSim Muscoloskeletal Modeling



isometric force  $[F^M_{max}(N) = CSA(cm^2)^*$  specific tension  $(N/cm^2)]$  for the erector spinae and multifidi muscle fibers with insertion and origins across L4-L5 [4]. Static optimization was executed with input of the segmental ROM obtained for the intact and the instrumented TLIF models for the various levels of muscle damage.

# Simulation of muscles and muscle forces on FE models

Our goal was to quantify effects of muscle damage at the L4-L5 (index level) and the adjacent segments (L3-L4, L5-S1). Hence the ribcage and thoracic segments were excluded from the final models to save computational time and conserve resources without affecting the outcome. The segmental muscle forces of interest obtained from the Open-Sim thoracolumbar model were incorporated into the FE lumbar spine model via connector forces attached to the sites of muscle origin and insertion. Specifically, the muscles fibers we incorporated were the psoas, quadratous lumborum (OL), iliocostalis lumborum pars lumborum (ILpl), iliocostalis lumborum pars thoracis (ILpt), longissimus thoracis pars lumborum (LTpl), longissimus thoracis pars thoracis (LTpt), Multifidus (MF), transverse abdominus (TA) and Iliocostalis Lumborum (IL). These muscles were implemented via connector forces from the site of origin and insertion for each muscle fiber. Certain muscles that had insertions present on distal body segments such as the thoracic spine or scapula, which were not present in our model, were modeled as coupled forces applied at the origin pointing to the site of muscle insertion. Eight total lumbar spine models were developed. Two of these models were the non-instrumented lumbar spine models for comparison to the instrumented models for flexion and extension. These intact models were input with intact muscle forces with no reductions and the same segmental lumbar ROM mentioned above applied as rotational boundary conditions present at each FSU to simulate the motion that the muscle forces would provide. The remaining six instrumented models included the 4.8%, 20.7%, and 90% CSA reductions for both flexion and extension. The instrumented lumbar models were loaded with reduced muscle forces as well as the same instrumented lumbar ROM mentioned above applied as rotational boundary conditions. A flowchart (Fig. 1) was constructed to assist the reader in understanding the complex nature of our modeling procedure.

The biomechanical outcomes of the intact model were compared to the MITLIF (4.8%), OSTLIF (20.7%) and complete damage (CDTLIF) (90%) models in terms of muscle forces, and annulus stresses for all levels of damage for flexion and extension. ROM of the intact and instrumented models was also compared. The nucleus pulposus was simulated

by using incompressible, isotropic, elastic / hexahedral elements (Young's Modulus = 9, Poisson's Ratio = 0.4999) (Table 1) making it behave as a fluid. The maximum intradiscal pressure (IDP) was recorded in the nucleus pulposa present at a specific node.

#### Results

#### **ROM**

As previously mentioned, all TLIF instrumented cases (MIT-LIF, OSTLIF, and CDTLIF) contained the same segmental lumbar ROM and were compared to the intact model. There were 9° of total lumbar extension. For extension (Fig. 3a), the L2-L3 level showed an increase of 2.3° with a negligible change at the cephalad (L3-L4) level in the instrumented models compared to intact. The caudal level (L5-S1) showed a decrease of 0.6° in the instrumented models compared to intact.

For flexion, there was  $16^{\circ}$  of total lumbar ROM in both intact and instrumented models. For flexion (Fig. 3b), a  $0.8^{\circ}$  increase was seen in the instrumented models compared to the intact model at the cephalad level. The L2-L3 level showed a  $2.3^{\circ}$  increase in the instrumented model compared to intact. The caudal level showed a  $0.6^{\circ}$  decrease in the instrumented model compared to intact.

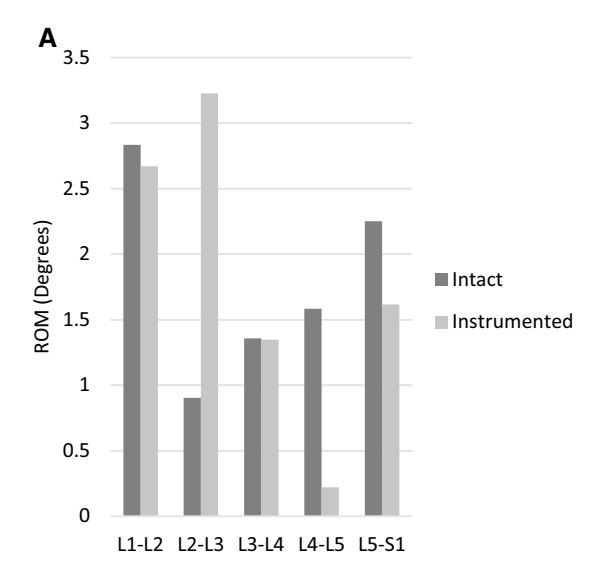
#### Muscle forces

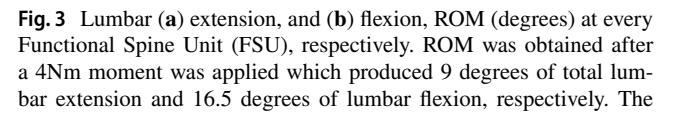
After the maximum isometric force was adjusted for each case, muscle forces in the lumbar spine were recorded using the OpenSim thoracolumbar model (Fig. 4) [8]. The changes in muscle forces were compared to the intact following 4.8%, 20.7%, and 90% CSA reduction in bilateral trunk muscles using the summation of individual muscle fibers for each muscle group.

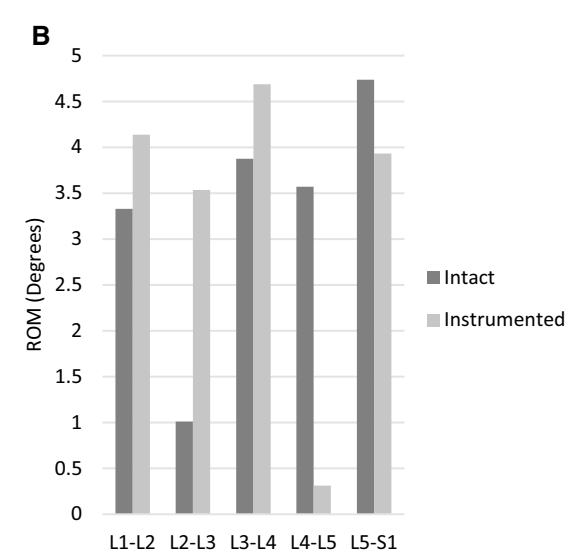
# 4.8% CSA reduction (MITLIF)

In extension (Fig. 4a), IL showed a 15% increase in muscle force when compared to the intact model. The psoas showed a 5% increase compared to intact. QL showed a 5% increase compared to the intact model. In flexion (Fig. 4b), the LTpL muscle force decreased by 6% compared to the intact model. A 9% decrease was seen in IL when comparing to the intact model. QL showed a 2% increase compared to intact. Other muscle groups in flexion remained relatively unchanged compared to intact.









instrumented (TLIF) model used the same overall ROM of 9 and 16.5 degrees applied at the L1 endplate to account for compensatory changes due to instrumentation [6]. The same instrumented ROM was used for each muscle reduction case

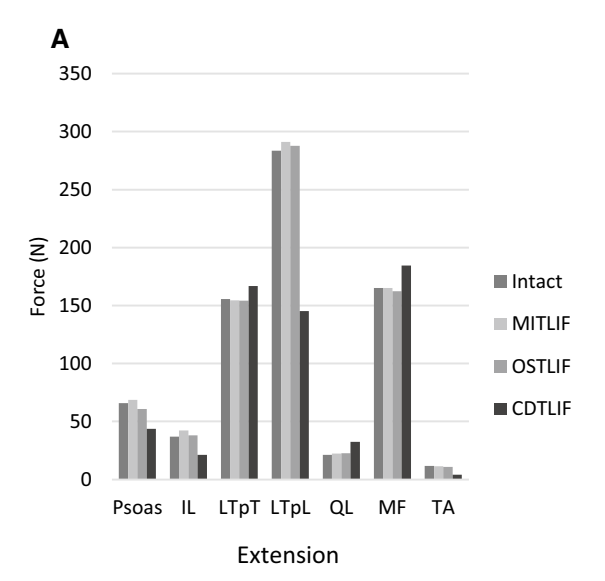
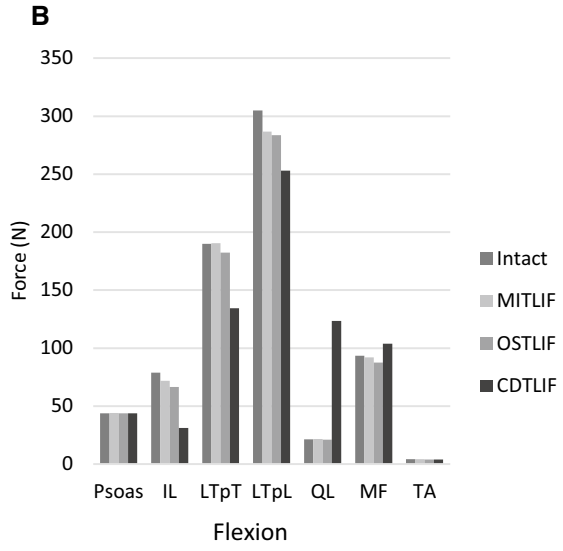


**Fig. 4** Trunk muscle force values obtained from the OpenSim simulation for intact and instrumented cases for (a) extension, and (b) flexion, respectively. Individual fibers were summed for each muscle group [psoas, Iliocostalis Lumborum (IL), longissimus thoracis pars thoracis (LTpT), longissimus thoracis pars lumborum (LTpL), quad-



ratous lumborum (QL), Multifidus (MF), and transverse abdominus (TA)]. MITLIF represents the 4.8% CSA reduction, OSTLIF represents the 20.7% CSA reduction, and CDTLIF represents the 90% CSA reduction

# 20.7% CSA reduction (OSTLIF)

In extension (Fig. 4a), QL showed a 7% increase in muscle force when compared to the intact model. Psoas showed a 7% decrease when compared to the intact model. TA showed an 8% decrease when compared to the intact

model. IL indicated a 3% increase compared to intact. In flexion (Fig. 4b), MF showed a decrease in muscle force by 6% compared to the intact model. LTpL showed a decrease of 7% when compared to the intact model. LTpT showed a decrease of 4% compared to intact. IL showed a decrease of 15% compared to the intact model. The QL and psoas groups remained unchanged compared to intact.



# 90% CSA reduction (CDTLIF)

In extension (Fig. 4a), psoas showed a 33% decrease compared to intact, similar decreases were seen in IL with 42%, LTpL with a decrease of 48% and TA with a decrease of 64% compared to intact. Major compensation occurred in the QL and MF groups with an increase of 52% and 12% compared to intact, respectively. LTpT also showed an increase of 7% compared to intact. In flexion (Fig. 4b), IL showed a 60% decrease when compared to the intact model. LTpT showed a 29% decrease compared to the intact model. LTpL showed a 17% decrease when compared to the intact model. Major compensation occurred in the MF and QL groups. MF showed an increase of 10% when compared to the intact model. QL showed a large 483% increase when compared to the intact model.

# **Intradiscal pressures (IDPs)**

Maximum IDPs were recorded for each TLIF case in flexion and extension (Fig. 5). The L4-L5 level was excluded as this was the site of fusion.

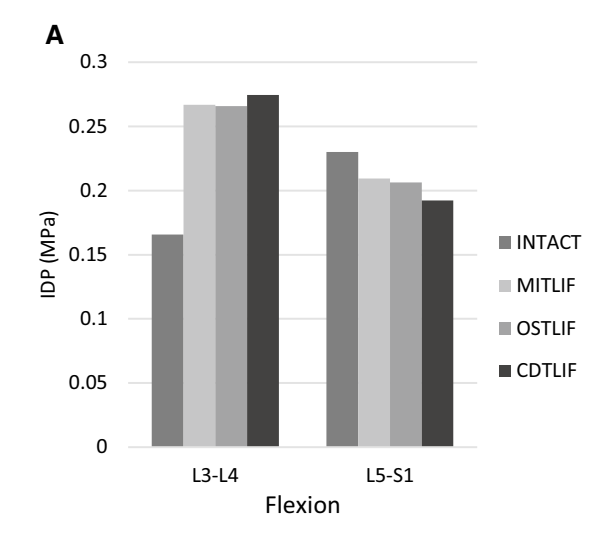
In flexion (Fig. 5a), IDPs increased by 60% in MITLIF and OSTLIF compared to the intact model and a negligible change was seen between the two at the cephalad level. CDTLIF showed a 65% increase compared to intact. The caudal level showed a 9%, 10%, and 16% decrease in

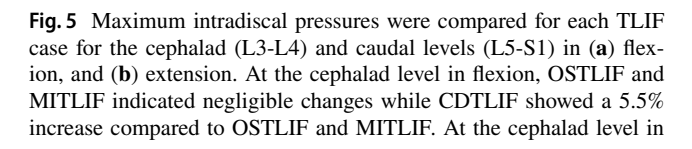
MITLIF, OSTLIF and CDTLIF compared to intact, respectively. In extension (Fig. 5b), IDP in MITLIF at the cephalad level showed a 50% increase while OSTLIF showed a 52% increase compared to intact. CDTLIF showed a 64% increase in IDP compared to intact. The caudal level showed negligible changes in MITLIF and OSTLIF, but a 25% decrease was seen in CDTLIF compared to intact.

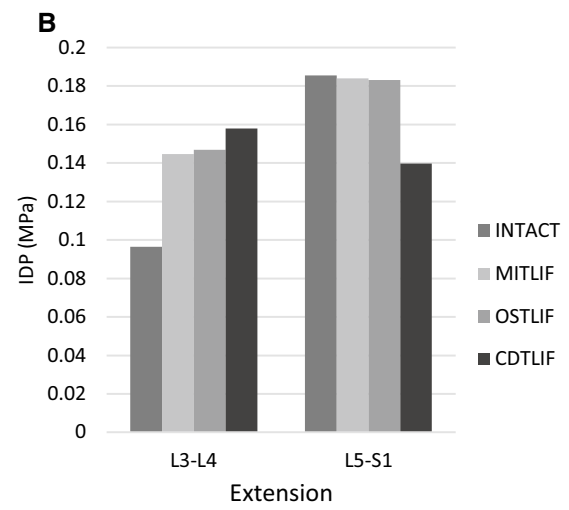
# **Annular fibrosa maximum stress**

Maximum annulus stresses were recorded for each TLIF case for flexion and extension (Fig. 6). The L4-L5 level was excluded as this was the site of fusion.

In flexion (Fig. 6a), a 108% increase was seen in MIT-LIF and OSTLIF compared to the intact model and a negligible change was seen between the two at the cephalad level. CDTLIF showed a 113% increase in annulus stress compared to the intact. The caudal level showed a 7% decrease for all TLIF cases. In extension (Fig. 6b), annulus stress in MITLIF at the cephalad level showed a 28% increase while OSTLIF showed a 29% increase compared to intact, respectively. CDTLIF showed a 37% increase in annulus stress compared to intact. The caudal level showed a 6%, 8%, and 43% decrease for MITLIF, OSTLIF, and CDTLIF compared to intact, respectively.

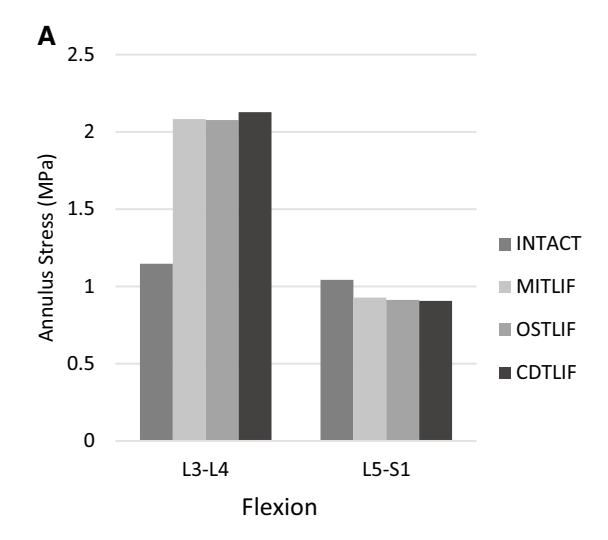






extension, OSTLIF showed a 2% increase compared to MITLIF while CDTLIF showed a 13% increase compared to MITLIF. Caudal levels in both flexion and extension indicated decreases as the level of damage increased





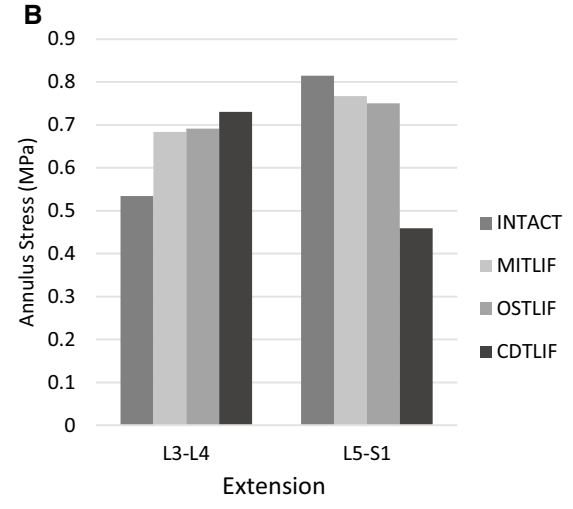


**Fig. 6** Annular stresses were compared for each TLIF case for the caudal and cephalad levels in (a) flexion, and (b) extension. At the cephalad level in flexion, negligible changes were seen comparing MITLIF to OSTLIF while a 5% increase was seen comparing CDT-LIF to MITLIF. The caudal level remained unchanged among the

TLIF cases in flexion. The cephalad level in extension indicated a 1% increase in OSTLIF compared to MITLIF while a 9% increase was seen in CDTLIF compared to MITLIF. The caudal level in extension indicated a decrease as the level of damage increased

# **Discussion**

The purpose of this study was to identify the changes in muscle forces and associated adjacent segmental soft tissue stresses after the paraspinal muscle fibers' CSA was bilaterally reduced by 4.8%, 20.7%, and 90% as a result of the potential muscle damage during the TLIF procedure and comparing it to the intact model. From the literature, 4.8% and 20.7% CSA reduction corresponds to the MIT-LIF and OSTLIF procedure, respectively [7]. 90% reduction (CDTLIF) resembles a situation in which muscle fibers are completely damaged. Our data suggests that preservation of posterior paraspinal muscles in MITLIF results in preservation of normal muscle forces compared to procedures that extensively damage the paraspinal muscles. Furthermore, our FE analysis indicated that due to the CSA changes in the muscle fibers, the annular stresses and IDPs at the adjacent levels had altered.

The results from the OpenSim simulation of flexion and extension indicated the major muscle force compensations occurring in different muscle groups for each motion. The results also suggested that MITLIF preserved paraspinal muscle forces which were most similar to intact. Flexion indicated that compensation in the MITLIF case occurred in the IL muscle group. The CDTLIF model indicated that compensation was occurring in the LTpT and MF muscle groups. A graded change was seen in the QL muscle group which also provided the largest compensation after paraspinal muscle CSA reduction at L4-L5. Extension showed that the QL and MF muscle groups also showed compensation, with the largest being in QL in CDTLIF. Furthermore,

graded changes were seen in the Erector Spinae muscles (IL, LTpT, LTpL) in both flexion and extension. These results are in agreement with Bresnahan's conclusion of a graded change seen in their study for the erector spinae fibers [4]. Other studies agree that the erector spinae provide co-contraction and spinal stability during flexion-extension, therefore it is vital to preserve these muscles during the TLIF procedure [4, 9, 10]. Clinical and biomechanical studies determined that the self-retaining retractors caused an increase in the intramuscular pressure and EMG muscle activity of the paraspinal muscles especially during increasing levels of CSA reduction in the paraspinal muscles [4, 7, 11]. Bresnahan's study confirmed a slight increase in the multifidus muscle activity as the CSA was reduced to 40% [4]. This is mirrored in our study at the multifidus and quadratus lumborum muscle group showed an increase in the CDTLIF case in both flexion and extension. These results are consistent with the biomechanical activity of the spine after iatrogenic muscle damage. This is due to the muscles compensating for the loss of force present in an adjacent muscle to keep the spine in equilibrium [12, 13].

Flexion showed higher ROM at the L2-L3 segment as well as the segment cephalad to the instrumentation (L3-L4) in the instrumented models. Extension showed higher ROM at the segment above the cephalad level (L2-L3) in the instrumented models. FE studies with ligamentous and traditional loads without muscle forces identified the presence of increased stresses in soft tissues as well as increased range of motion (ROM) adjacent to the site of instrumentation [14–16]. Our study indicated similar large intradiscal pressure increases at the cephalad segment when comparing



the MITLIF, OSTLIF and CDTLIF cases to the intact case in both flexion and extension. Our data is consistent with the previous studies. As the level of muscle damage increased in extension, the cephalad levels showed slight increases in IDP and annulus stress from MITLIF to OSTLIF with a further increase seen in the CDTLIF case. Flexion indicated negligible changes in comparing the MITLIF to OSTLIF, though CDTLIF showed an increase in both IDP and annulus stress. Both models showed decreases at the caudal segment in both IDP and annulus stress. This indicates that the soft tissues in fact respond to changes in muscle loading, especially when CSA reduction is occurring in the TLIF procedure.

The findings of the current study may indicate the potential for further change to adjacent segment's soft tissue after instrumentation and paraspinal muscle retraction [14, 16–22]. This alteration to soft components of the lumbar spine after instrumentation and muscle manipulation that cause iatrogenic muscle damage may further exacerbate lower back pain in patients who sought to correct initial back pain through the TLIF procedure [15]. This observation may indicate muscle damage's role on the cephalad and caudal adjacent segment during flexion-extension.

As studied by Panjabi [6], it was proposed that the alteration of the spine specimens at one or more level will redistribute adjacent intervertebral motions to allow for the patient to perform pre-alteration total motion. For example, a patient post-operatively may wish to move the spine in a similar way as they did pre-operatively such as bending over to tie their shoes. Similar studies have shown that singlelevel fusions similar to what was performed in the scope of this study may produce compensatory changes and additional stresses in the adjacent segments to the fusion [25]. Therefore, it was imperative that our methodology implemented the "hybrid protocol" as outlined in the methods section (Fig. 2) by implementing the same overall ROM before and after instrumentation to understand the effect of instrumentation and changes in segmental ROM on adjacent levels. The implementation of this protocol may have attributed to the cephalad and caudal increases in stress when comparing the intact model to the instrumented models. Limitations exist with this protocol, including the uncertainty on whether a patient truly experiences the same overall lumbar ROM post-operatively. Another limitation includes the three-dimensional coupled motions that would occur in axial rotation and lateral bending which would be different in the intact and instrumented models, making it difficult to match the exact motion which is why only flexion-extension was studied.

Our FE models contain a number of simplifications. First, thoracic segmental ROM for the intact and instrumented ribcage models was assumed to be the same, though was only used as OpenSim required these thoracic motions to output accurate lumbar muscle forces. This ROM was

excluded from the final lumbar intact and instrumented models. Additionally, when loading muscles onto the FE models, displacement control was applied at each FSU for every model to allow the spine to perform flexion-extension that the 4Nm moment created; the muscle forces did not produce the motions. Another limitation was assuming that all levels of muscle reduction produced the same segmental ROM. This may not be the case *in-vivo* as the degree of muscle damage may further affect segmental motions in the spine. Furthermore, the simulation of muscle forces in the FE models are a simplification of what is seen *in-vivo*. Simple connector and coupled forces were applied. A future model with muscle fibers with correct material properties and articulation should be explored in the future.

The scope of this study was to identify graded changes in the stresses of the FE model after varying levels of muscle CSA reduction.

# **Conclusion**

This study provides a quantifiable investigation of the adjacent segment changes seen after iatrogenic muscle damage on the lumbar spine during the TLIF procedure in a finite element model. As minimally invasive surgeries become more prevalent with an effort to preserve musculature and soft tissue architecture, biomechanical data is becoming more valuable. This study provides further insight of the benefits of MITLIF to the traditional open procedure and reasoning to believe that paraspinal muscle damage causes graded changes in the adjacent segments of the TLIF fusion which can lead to further postoperative back pain. Our methodology provides a novel way of incorporating muscle forces onto the finite element model that has the ability to analyze muscle damage postoperatively for long segment fusions, comparisons of minimally invasive procedures, and the effect of physiotherapeutic muscle strengthening. We intend on utilizing our approach to compare cases like Anterior Lumbar Interbody Fusion (ALIF) with and without percutaneous PSF and TLIF with unilateral PSF and bilateral PSF through Kambin's triangle. These studies will help direct surgeons in their operative plan.

Acknowledgements The work was supported in part by NSF Industry/ University Cooperative Research Center at The University of California at San Francisco, CA, The Ohio State University, Columbus, Ohio, The University of Toledo, Toledo, OH (www.nsfcdmi.org) and AO Foundation.

# References

 Mobbs RJ, Phan K, Malham G, Seex K, Rao PJ (2015) Lumbar interbody fusion: techniques, indications and comparison of interbody



- fusion options including PLIF, TLIF, MI-TLIF, OLIF/ATP. LLIF and ALIF J Spine Surg (Hong Kong). https://doi.org/10.3978/j.issn. 2414-469X.2015.10.05
- Davis H (1994) Increasing rates of cervical and lumbar spine surgery in the United States, 1979–1990. Spine. https://doi.org/10.1097/ 00007632-199405001-00003
- Rahman M, Summers L, Richter B, Mimran R, Jacob R (2008) Comparison of techniques for decompressive lumbar laminectomy: the minimally invasive versus the "classic" open approach. Minim Invasive Neurosurg. https://doi.org/10.1055/s-2007-1022542
- Bresnahan L, Fessler RG, Natarajan RN (2010) Evaluation of change in muscle activity as a result of posterior lumbar spine surgery using a dynamic modeling system. Spine (Phila Pa 1976). https://doi.org/ 10.1097/BRS.0b013e3181e45a6e.
- Watkins R, Williams L, Watkins R, Ahlbrand S, Garcia R, Karamanian A et al (2004) Stability provided by the sternum and rib cage in the thoracic spine. Spine J. https://doi.org/10.1016/j.spinee.2004.05.003
- Panjabi MM (2007) Hybrid multidirectional test method to evaluate spinal adjacent-level effects. Clin Biomech. https://doi.org/10.1016/j.clinbiomech.2006.08.006
- Hyun SJ, Kim YB, Kim YS, Park SW, Nam TK, Hong HJ et al (2007) Postoperative changes in paraspinal muscle volume: comparison between paramedian interfascial and midline approaches for lumbar fusion. J Korean Med Sci. https://doi.org/10.3346/jkms. 2007.22.4.646
- Bruno AG, Bouxsein ML, Anderson DE (2015) Development and validation of a musculoskeletal model of the fully articulated thoracolumbar spine and rib cage. J Biomech Eng. doi 10(1115/1):4030408
- Cholewicki J, Panjabi MM, Khachatryan A (1997) Stabilizing function of trunk flexor-extensor muscles around a neutral spine posture. Spine(Phila Pa 1976) 22(19):2207–2212
- Granata KP, Marras WS (2000) Cost-benefit of muscle cocontraction in protecting against spinal instability. Spine (Phila Pa 1976) 25(11):1398–1404. https://doi.org/10.1097/00007632-20000 6010-00012
- Kim DY, Lee SH, Sang KC, Lee HY (2005) Comparison of multifidus muscle atrophy and trunk extension muscle strength: Percutaneous versus open pedicle screw fixation. Spine (Phila Pa 1976) 30(1):123–129. https://doi.org/10.1097/01.brs.0000148999.21492. 53
- Barrangou R, Horvath P, Jinek M, Chylinski K, Fonfara I, Hauer M et al (2014) Degeneration and mechanics of the segment adjacent to a lumbar spine fusion: a biomechanical analysis. Cell. https://doi.org/10.1016/j.cell.2009.01.043
- White AA, Panjabi MM (1978) Clinical biomechanics of the spine. Lippincott, Philadelphia
- Cao L, Liu Y, Mei W, Xu J, Zhan S (2020) Biomechanical changes of degenerated adjacent segment and intact lumbar spine after lumbosacral topping-off surgery: a three-dimensional finite element analysis. BMC Musculoskelet Disord. https://doi.org/10.1186/ s12891-020-3128-5
- Perez-Cruet MJ, Hussain NS, White GZ, Begun EM, Collins RA, Fahim DK et al (2014) Quality-of-life outcomes with minimally invasive transforaminal lumbar interbody fusion based on longterm analysis of 304 consecutive patients. Spine (Phila Pa 1976) 39(3):E191–E191. https://doi.org/10.1097/BRS.000000000000000078
- Ames CP, Acosta FL, Chi J, Iyengar J, Muiru W, Acaroglu E et al (2005) Biomechanical comparison of posterior lumbar interbody fusion and transforaminal lumbar interbody fusion performed at 1 and 2 levels. Spine (Phila Pa 1976) 30(19):E562–E566. https://doi. org/10.1097/01.brs.0000180505.80347.b1
- Hussain M, Nassr A, Natarajan RN, An HS, Andersson GBJ (2013) Biomechanics of adjacent segments after a multilevel cervical corpectomy using anterior, posterior, and combined anterior-posterior

- instrumentation techniques: a finite element model study. Spine J. https://doi.org/10.1016/j.spinee.2013.02.062
- Tang S, Rebholz BJ (2011) Does anterior lumbar interbody fusion promote adjacent degeneration in degenerative disc disease?
   J Orthop Sci, A finite element study. https://doi.org/10.1007/s00776-011-0037-3
- Tang S (2015) Comparison of posterior versus transforaminal lumbar interbody fusion using finite element analysis. Influence on adjacent segmental degeneration. Saudi Med J. https://doi.org/10.15537/smj.2015.8.11759
- Weinhoffer SL, Guyer RD, Herbert M, Griffith SL (1995) Intradiscal pressure measurements above an instrumented fusion: a cadaveric study. Spine(Phila Pa 1976) 20(5):526–531
- Jiang S, Li W (2019) Biomechanical study of proximal adjacent segment degeneration after posterior lumbar interbody fusion and fixation: a finite element analysis. J Orthop Surg Res. https://doi.org/ 10.1186/s13018-019-1150-9
- Kushchayev SV, Glushko T, Jarraya M, Schuleri KH, Preul MC, Brooks ML et al (2018) ABCs of the degenerative spine. Insights Imaging. https://doi.org/10.1007/s13244-017-0584-z
- Shah A, Kumaran Y, Zavatsky JM, McGuire R, Serhan H, Goel VK (2019) Development of a Novel Finite Element Model of a Thoracolumbar spine and Ribcage to Study the Effects of Musculoskeletal Disorders. Biomed Eng Soc Annu Meet 2019.
- Shah A, Lemans JVC, Agarwal A, Kruyt MC, Serhan H, Agarwal A, Zavatsky J, Goel VK (2019): Spinal Balance/Alignment Clinical Relevance and Biomechanics. ASME J Biom. Engrg., 141(7), 070805-1 14. https://doi.org/10.1115/1.4043650
- Yoshimoto H, Ito M, Abumi K, Kotani Y, Shono Y, Takada T, Minami A (2004) A retrospective radiographic analysis of subaxial sagittal alignment after posterior C1–C2 fusion. Spine 29(2):175– 181. https://doi.org/10.1097/01.BRS.0000107225.97653.CA
- Ivanov AA, Kiapour A, Ebraheim NA, Goel V (2009) Lumbar fusion leads to increases in angular motion and stress across sacroiliac joint: a finite element study. Spine 34(5):E162–E169. https:// doi.org/10.1097/BRS.0b013e3181978ea3
- Lindsey, D. P., Kiapour, A., Yerby, S. A., & Goel, V. K. (2015) Sacroiliac joint fusion minimally affects adjacent lumbar segment motion: a finite element study. International journal of spine surgery, 9, 64. https://doi.org/10.14444/2064
- Joukar A, Shah A, Kiapour A, Vosoughi AS, Duhon B, Agarwal AK, Elgafy H, Ebraheim N, Goel VK (2018) Sex specific sacroiliac joint biomechanics during standing upright: a finite element study. Spine 43(18):E1053–E1060. https://doi.org/10.1097/BRS.0000000000 002623
- Panjabi MM, Oxland TR, Yamamoto I, Crisco JJ (1994) Mechanical behavior of the human lumbar and lumbosacral spine as shown by three-dimensional load-displacement curves. JBJS 76(3):413

  –424
- Jones AD. (2013) Biomechanical and finite element analyses of alternative cements for use in vertebral kyphoplasty. Dissertation, University of Toledo.
- Gerber, J. M. (2015) Biomechanical evaluation of facet bone dowels in the lumbar spine. Dissertation, University of Toledo
- Palepu, V. (2013) Biomechanical effects of initial occupant seated posture due to rear end impact injury. Dissertation, University of Toledo.
- Vosoughi AS, Joukar A, Kiapour A, Parajuli D, Agarwal AK, Goel VK, Zavatsky J (2018) Optimal Satellite Rod Constructs to Mitigate Rod Failure Following Pedicle Subtraction Osteotomy (PSO): A Finite Element Study. Spine J 5(5):931–941

**Publisher's Note** Springer Nature remains neutral with regard to jurisdictional claims in published maps and institutional affiliations.

